CCFE
CULHAM CENTRE FOR FUSION ENERGY

UK Atomic Energy Authority

UKAEA-CCFE-PR(22)16

M. Rubel, A. Widdowson, L. Dittrich, S. Moon, A. Weckmann, P. Petersson, JET Contributors

Application of Ion Beam Analysis in Studies of First Wall Materials in Controlled Fusion Devices

Application of Ion Beam Analysis in Studies of First Wall Materials in Controlled Fusion Devices

M. Rubel, A. Widdowson, L. Dittrich, S. Moon, A. Weckmann, P. Petersson, JET Contributors

This is a preprint of a paper submitted for publication in Physics

physics

MDPI

33Article

Application of Ion Beam Analysis in Studies of First Wall Materials in Controlled Fusion Devices

M. Rubel[1], A. Widdowson[2], L. Dittrich[1], S. Moon[1], A. Weckmann[1], P. Petersson[1], JET Contributors*

[1]KTH Royal Institute of Technology, Fusion Plasma Physics, Stockholm, Sweden

[2]Culham Centre for Fusion Energy, Abingdon, United Kingdom

*See the list of authors: J. Mailloux, 28th IAEA Fusion Energy Conference 2020 (May 2021)

Abstract: The contribution provides a concise overview of ion beam analysis methods and procedures in studies of materials exposed to fusion plasmas in controlled fusion devices with magnetic confinement. An impact of erosion-deposition processes on the morphology of wall materials is presented. In particular, results for deuterium analyses are discussed. Underlying physics, advantages and limitations of methods are addressed. The role of wall diagnostics in studies of material migration and fuel retention is explained. A brief note on research and handling of radioactive and beryllium-contaminated materials is also given.

Keywords: Ion beam analysis, plasma facing materials, hydrogen isotopes, JET, TEXTOR

Citation: Lastname, F.; Lastname, F.; Lastname, F. Title. *Physics* **2021**, *3*, Firstpage–Lastpage. https://doi.org/10.3390/xxxxx

Received: date
Accepted: date
Published: date

1. Introduction

The ultimate goal of research in the field of controlled thermonuclear fusion of light nuclei is to construct and operate an energy generating system for sustainable electricity production. The development involves a broad range of scientific and engineering challenges arising from the fact that under terrestrial conditions thermonuclear fuel must be surrounded by walls of a vacuum vessel. This applies to all confinement concepts considered for a fusion reactor: (a) inertial confinement based on the irradiation of a pellet with hydrogen isotopes by intense photon (laser) or ion beams; (b) plasma confined by strong magnetic field of the order a few tesla in devices called tokamaks (from Russian: *toroidal chamber with magnetic coils*) or stellarators. This work deals with materials from tokamaks.

Over eighty experimental controlled fusion devices (CFD) representing various plasma confinement concepts, magnetic and inertial, are active world-wide. The world's largest, operated with many modifications since June 1983, is the Joint European Torus (JET), a tokamak in the United Kingdom [1]. The next-step device of a reactor-class is under construction in France: ITER, meaning "*The Way*" in Latin. Lessons learnt from the construction and operation of earlier devices have been taken into account in the ITER design. It should be stressed that each tokamak or stellarator, operated either in the past or at present, has had specific scientific and technological missions. One of them is the test of plasma-facing materials (PFM) and components (PFC) to ensure reliable performance under extreme conditions of the nuclear environment [2-5].

Fusion processes considered for the reactor operation involve deuterium (D, d), tritium (T, t) and helium-3 (^{3}He) as reactions' substrates, while hydrogen (protium H, p), ^{4}He (alpha particle) and neutrons are among products.

$$D + D \rightarrow T\ (1.01\ MeV) + H\ (3.03\ MeV) \quad (1a)$$

$$D + D \rightarrow {}^3He\ (0.82\ MeV) + n\ (2.45\ MeV) \quad (1b)$$

$$D + {}^3He \rightarrow \alpha\ (3.67\ MeV) + H\ (14.69\ MeV) \quad (2)$$

$$D + T \rightarrow \alpha\ (3.52\ MeV) + n\ (14.06\ MeV) \quad (3)$$

$$T + T \rightarrow {}^4He\ (3.77\ MeV) + 2n\ (7{,}53\ MeV) \quad (4)$$

The branching ratio of Reactions 1(a) and 1(b) is around one.

The main point in selecting a process for a reactor-class machine is the reaction rate and the availability or possibility of obtaining fuel. Present-day experimental magnetic CFD use deuterium fuel, Reactions 1(a) and (b), which is available in nature: around 34 g in 1 m^3 of water. The practical use of Reaction 2 in reactor technology is not possible because of: (i) unavailability of ^{3}He in large quantities; (ii) very high energy release (Q value) to which the wall materials would be exposed. That reaction, however, is very often used in ion beam analysis (IBA) of PFM, as addressed in Chapter 5. The comparison of cross-sections indicates the D – T reaction as the most effective from the energy point of view. The maximum is around 70 keV (700 000 000 K) of D energy but high D-T reactivity is reached already at 20 keV. Maxima of other reactions are above 120 keV [6]. The D-T fusion

results in the emission of a 3.5 MeV alpha particle and a fast neutron carrying 14.1 MeV. The role of energetic alphas is to heat the plasma. It implies that PFC must eventually extract the radiated power, while the thermalised ^{4}He atoms are removed as ash of the fusion process. Neutrons pass PFM and interact with structural and functional materials of the reactor wall. Their energy is to be deposited in the lithium-containing blanket. Reactions with lithium produce tritium indispensable for the reactor operation [7,8]. The role of neutrons and a neutron-induced effects have been decribed elsewhere [9,10],

2. Plasma - wall interactions and wall materials

This work deals with the plasma impact on wall materials. They are modified by a set of processes known as plasma-material interactions (PMI) or plasma-wall interactions (PWI) [3,11-13]. The wall is irradiated by particles escaping the plasma: electrons, ions at different charge state and, by energetic neutrals. Some incoming particles are reflected, while others are implanted thus changing the surface region composition. The implanted species may be: (i) released (desorbed) after certain time either in the original or chemically changed form; this - including the reflection - is called recycling; (ii) trapped and reside in the solid either as a sole implant (e.g. interstitial) or chemically bound; this is called retention. In either case, particles incoming from the plasma transfer a fraction of their energy to the wall material thus causing its erosion. The main process is physical sputtering which occurs for all projectile–target combinations [14], unless the projectile energy is below the energy threshold for a given system [15]. The erosion is enhanced when the interaction involves chemical reaction(s) leading to the formation of volatile compounds with H isotopes or plasma impurities, e.g. O or N. Other erosion channels are related to arcing and those caused by high heat loads resulting in cracking, melting, boiling, evaporation and splashing of the molten material.

All eroded and other (e.g. from leaks or intentionally seeded to the torus) plasma impurity atoms are instantly ionised and then travel along the magnetic field lines until they are pumped-out or are re-deposited in the torus at the place located close or far away from the place of origin. Upon re-deposition plasma impurities are co-deposited together with H isotopes producing so-called co-deposits. Their properties are different from from those characteristic for the original wall materials. Co-deposition is decisive for fuel inventory which must be strictly controlled; the in-vessel T retention in ITER is limited to 700 g [16,17]. The formation of co-deposits has a major impact on all surface properties of PFC and, also on in-vessel plasma diagnostic components. In addition, disintegration or exfoliation of co-deposits generates dust [18,19]. Fuel inventory and dust formation are crucial for the safety and economy in the D-T reactor operation.

The list of required PFM properties comprise: high thermal conductivity, resilience to thermal shocks, compatibility with vacuum, high melting point, low activation by neutrons, low reactivity with H isotopes, O, N towards formation of volatile products, low sorption of H isotopes to minimize in-bulk fuel retention, low sputter erosion yield. There is no ideal material fulfilling such requirements. The search for a suitable material started already in late sixties of the 20th century when detrimental effects of PWI on plasma

performance had been recognized. When saying "detrimental" one has to stress simultaneously that PWI processes are – first of all – unavoidable because plasma surrounding by the wall is a pre-requisite. They are also necessary to thermalize and remove He and, to extract neutron energy in the reactor blanket with Li compounds.

Over the years a large variety of materials had been considered and tested as candidates, but eventually only a few of them have been used for wall components under fusion environment. The status until the end of the 20th century is summarized in Table 1 of reference [3]. The focus has been on carbon (C) in the form of graphite or various carbon fibre composites (CFC), tungsten (W) and beryllium (Be). For many years carbon was the main wall material in most devices [3,13,20-23]]. Its power-handling capabilities are excellent, but the affinity to hydrogen isotopes results in chemical erosion (hydrocarbons) and, in a consequence, formation of co-deposited layers with unacceptable fuel inventory [17,20,24-26]. The original ITER plan was to use all three materials in various regions of the reactor dependent on the power load. However, such material combination had never been tested together under fusion conditions. A large-scale test of the all-metal wall was decided in year 2004: ITER-Like Wall Project at the JET tokamak (JET-ILW) [5]. Carbon components (JET-C operated till October 2009) were replaced by Be on the main chamber wall and W in the divertor [5,27]. A combined image in Figure 1 shows components of JET-C (left) and JET-ILW (right). The image also reveals complexity of the plasma-facing wall with several types of limiters in the main chamber and the arrangement of tiles in the divertor. Details about respective structures can be found in [28] for JET-C and in [29-33] for the JET-ILW Project which involved a very broad R&D programme. The operation started in 2011 indicated a significant decrease of fuel retention [34-36]. This was followed by the decision of the ITER Organisation to abandon carbon PFC, i.e. to use only W in the divertor and Be in the main chamber [37].

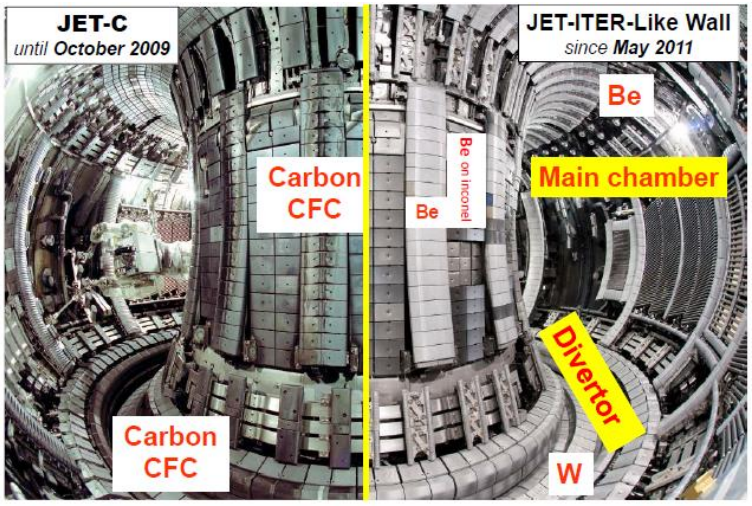

Fig. 1. Toroidal view into the vacuum vessel of the JET tokamak. Left: CFC limiter and divertor tiles in JET-C. Right: ITER-Like Wall with bulk beryllium limiters and Be-coated Inconel of the inner wall cladding in the main chamber and, bulk tungsten in the divertor base and W-coated CFC tiles in the inner and outer divertor legs. All details can be found in [5].

3. The role of analysis in studies of reactor materials

Research in the field of PWI comprises three fundamental elements (i) experiments in CFD and in relevant PWI simulators; this strand includes material testing; (ii) ex-situ and in-situ analysis of wall components and erosion – deposition probes called also wall probes; (iii) modelling. Therefore, analysis is not an isolated activity but an integral part of the entire research program. Its main role is to help understanding processes which modify materials, lead to the degradation of their properties and, to the contamination of fusion plasmas by species eroded from the wall. The analysis must provide data for the assessment of erosion–deposition pattern in the entire vessel and, by this, for modelling of material transport. To answer fundamental questions on *what* has happened and *why* in order to plan *how* to deal with a given problem, one has to possess knowledge on specific points regarding material migration, i.e. the location of erosion and deposition zones, the level of fuel inventory and, the PWI impact on plasma diagnostic components. The study requires both (i) materials retrieved from the torus (a properly selected set of PFC tiles, wall probes and dust particles) and (ii) laboratories with specialized apparatus and capabilities of handling reactor materials contaminated for instance by Be and T [38].

3.1 Species to be analysed

The overall aim is to obtain a comprehensive overview of material migration. For that reason, analyses are carried out for all types of species present in the torus including those which were either deliberately or accidently introduced to the torus. The basic list starts with the hydrogen isotopes (H, D, T) and ^{4}He, Be, C, O impurity, steel and/or Inconel® constituents of the vacuum vessel material (Fe, Cr, Ni, Mn, Mo) and, it finishes with tungsten. In practice, the number of species of interest is much longer because one has to determine gases injected to the torus for plasma edge cooling (N, Ne, Ar, Kr, Xe), auxiliary heating with radio frequency (^{3}He), tracers in material migration studies (^{10}Be, ^{10}B, ^{11}B, ^{13}C, ^{15}N, ^{18}O, ^{21}Ne and F in the form as Mo or W hexafluorides), elements for wall conditioning (Li, B, Si) and others used for instance in marker tiles (Ta, Re).

4.2 Tiles: limiters and divertor

Figure 2 shows a number of wall tiles retrieved from the JET and TEXTOR tokamaks after long-term experimental campaigns. (*Note: TEXTOR was in operation 1982-2013*.) This collection demonstrates both the variety of shape/size/weight of components and surface characteristics after the exposure to plasma. All these features have a serious impact on the analytical procedure. Colourful patterns prove not uniform surface composition attributed to erosion-deposition processes. Therefore, there is a need for mapping the distribution of various species over large surfaces. This calls for analysis stations with large chambers and manipulators with a long long-travel to avoid sectioning of tiles, unless cutting or cleaving is necessary either for other studies (metallography, microscopy) or to reduce the level of activity to be handled in the case of samples containing for instance high amounts of tritium [25,26,38].

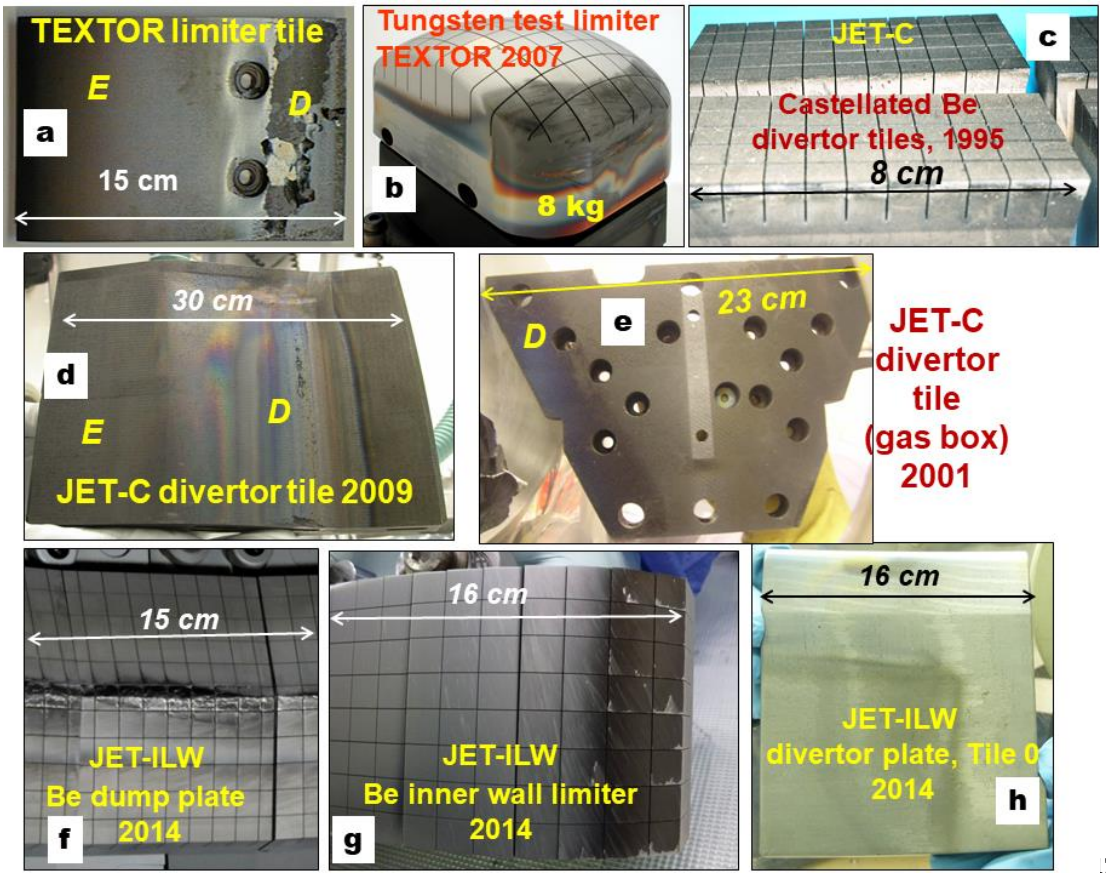

Fig. 2. Plasma-facing components from TEXTOR and JET tokamaks: (a) graphite plate from the toroidal belt pump limiter; (b) castellated test limiter made of bulk W; (c) Castellated Be tiles from Mk-I-Be divertor; (d) CFC tile from Mk-II divertor; (e) CFC tile from the septum structure of the Mk-II Gas Box divertor; (f) castellated upper dump plate (upper divertor) made of bulk Be; (g) castellated tile of the inner wall guard limiter made of bulk Be; (h) W-coated CFC tile from the upper part of the inner divertor. (E) and (D) denote erosion and deposition zones on respective PFC.

4. Analysis methods

Nearly fifty different techniques have been applied to obtain the most fundamental and very specific information on the change of PFM/PFC morphology under the plasma impact: structure (surface and bulk) and composition (elemental, isotopic, chemical). There is no single method capable of addressing all these points. The most efficient set of tools is to be selected, i.e. methods for sensitive and selective determination of the content and distribution (lateral and in-depth) of hydrogen isotopes and several light and heavier elements listed in Paragraph 3.1. A review of techniques was already given in earlier articles [39,40]. High speed in analysis is also important when probing hundreds of points over large areas of PFC. Such criteria are met by ion beam analysis (IBA) methods, especially accelerator-based techniques [39-43]. The principle of IBA is the irradiation of a solid with a monochromatic collimated ion beam followed by energy and/or mass analysis of species leaving the target. It is exemplified in Figure 3 showing the emission of different signals under ion irradiations: sputtered ions and neutrals (monoatomic or molecular),

scattered primary ions, recoiled particles, photons originating from electronic and nuclear excitations, a variety of nuclear reaction products including neutrons. Taking into account a broad energy range (a few eV to tens of MeV) and various types of the primary beam (e.g. H^+, D^+, $^3He^+$, $^4He^+$, $^{12}C^{3+}$, $^{127}I^{9+}$) the number of combinations is huge.

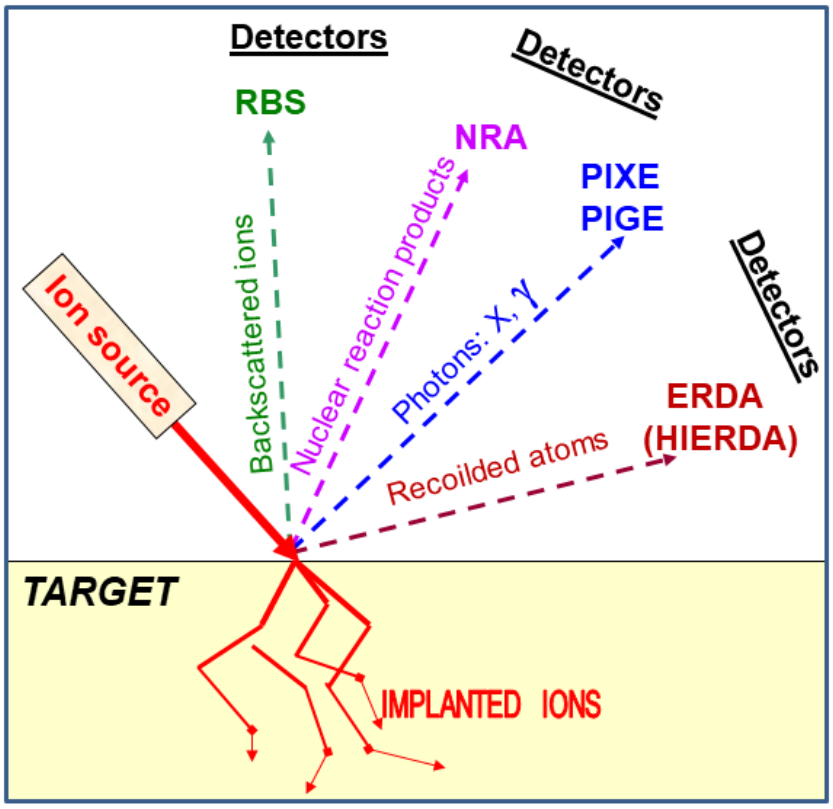

Fig. 3. Ion – surface interactions: phenomena underlying different analysis methods.

The palette of accelerator-based IBA for practical use in studies of reactor materials comprises Rutherford backscattering spectroscopy (RBS), particle induced X-ray emission (PIXE) and nuclear reaction analysis (NRA) both with a standard beam (diameter 0.6 - 1 mm) or micro- beam (⊚-RBS, ⊚-NRA, ⊚-PIXE with lateral resolution in the range 0.5 - 20 μm). It is stressed that NRA offers a large number of reactions to ensure proper selectivity in the detection of respective low-Z isotopes. Such analyses are also carried out by means of time-of-flight high-energy elastic recoil detection (ToF-HIERDA) and accelerator mass spectrometry (AMS). Research capabilities are enhanced by new developments of apparatus and codes. For instance, deuterium retention studies have been extended by using high energy ^3He (up to 6 MeV) [44], a dedicated chamber has been constructed to enable in-situ studies of dynamic processes [45], while new detection system has led to the improved mass resolution [46]. There are continuous updates of the SIMNRA code for spectra analysis [47]. A comprehensive account on IBA facilities for studies of PFC is in [43]. A number of examples, especially in fuel retention studies, will be presented below.

5. Fuel retention studies

As mentioned in Chapters 2 and 3, the determination of hydrogen isotopes in PFC belongs to top priorities. It is motivated by the need to assess the inventory in a D-T reactor. Studies are concentrated on deuterium, i.e. the main fuel of present-day devices. Application of NRA based on a $^{3}He^{+}$ beam is the most efficient approach to determine D together with other low-Z species such as Be and C by detecting the energy spectrum of protons emerging from the following reactions: $^{3}He(d,p)^{\circledcirc}$, $^{3}He(^{9}Be,p)^{11}B$, $^{3}He(^{12}C,p)^{14}N$. A spectrum obtained with a 2.5 MeV $^{3}He^{+}$ beam is in Figure 4. In addition to protons from the above listed reactions there is also a feature associated with the $^{3}He(^{13}C,p)^{15}N$ reaction. The analysis was carried out on a divertor tile from JET-C after material migration experiments employing a ^{13}C-labeled $^{13}CH_4$ as a tracer to determine the carbon transport to so-called remote areas [28,48,49]. These are regions outside the direct plasma line-of-sight, for instance shadowed areas in the inner and outer divertor.

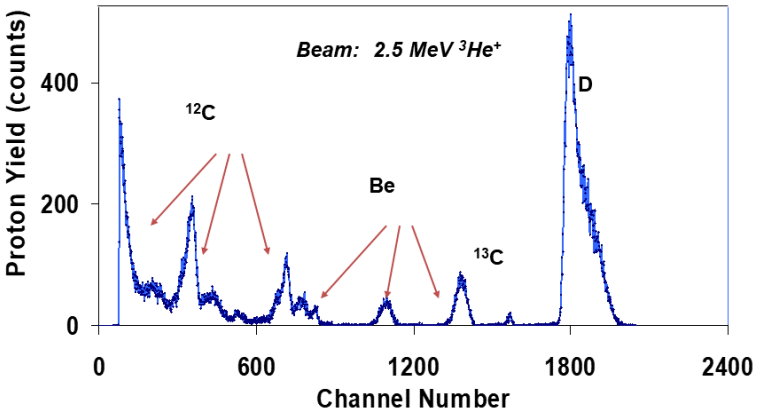

Fig. 4. *^{3}He-NRA spectrum for a divertor tile from JET-C showing features of carbon (^{12}C and ^{13}C), Be and D.*

Very detailed D analyses performed on material retrieved from JET-ILW, both PFC and wall probes from shadowed regions in the divertor, have consistently shown the decrease of retention by a factor of 10-15 in comparison to the situation in JET-C [50-58]. Also the co-deposit thickness was decreased when the direct carbon source on PFC was eliminated. For instance, on wall probes (test mirrors) from the inner divertor the thickness after a full experimental campaign (~ 20 h of plasma operation) dropped from around 20 μm in JET-C to less than 1 μm in JET-ILW [58]. To obtain a more complete retention pattern in JET-ILW analyses were to be performed: (i) inside the grooves of castellated Be limiters, see Figure 2 (f-g) and (ii) on the Be-coated Inconel tiles of the inner wall cladding, for details see the right side of Figure 1.

All plasma-facing components in ITER will be castellated because such structure of tiles is deemed as the best solution to ensure thermo-mechanical durability and integrity of materials under high heat flux loads. However, 0.4 mm wide grooves of castellation may act as shadowed zones of PFC in which co-deposits rich in fuel can be formed. Therefore, side surfaces located in the grooves are to be studied. The motivation for studies of the JET castellated structures is related to the fact that nearly 2 000 000 such surfaces will be in ITER in the Be panels in the main chamber and in the W divertor. The analysis has been

possible only after cutting the Be tiles using special procedures and applying μ-NRA to determine the deposition pattern [59]. Figure 5 (a-c) show respectively the surface inside the castellation, the geometry of the castellated block and, the deposition profiles of D and trace quantities of metallic plasma impurities. The D presence is detected only in narrow deposition belts 0.5-1.3 mm deep into the gap. In most cases (around 100 studied surfaces) the D content has been below $1x10^{18}$ cm^{-2} and, in neither case it exceeded $3x10^{18}$ cm^{-2}. Such quantities are considered as very small from the point of view of retention. However, Be limiters in JET have nearly 180 000 surfaces in the gaps (7.5 km long) thus the impact on the total retention must be considered. The total D content has been estimated in the range from 0.7×10^{22} to 14.2×10^{22} in the castellation. The upper value is on a similar level as the retention determined reported in [50] on the PFS of the limiters, thus indicating that the deposition in the grooves of castellation is not decisive for the entire deuterium inventory; most D is retained in the divertor. However, the contribution from the castellation cannot be neglected in the total count.

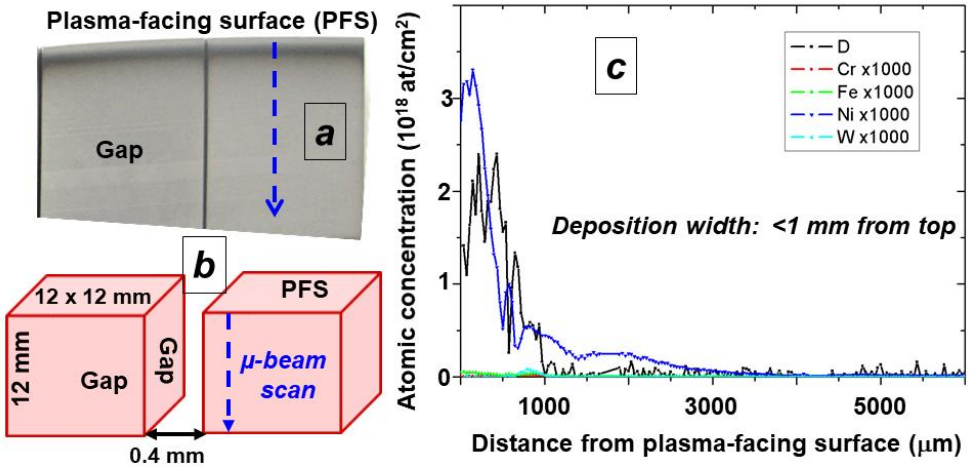

Fig. 5. Deposition inside castellated Be limiters from JET-ILW: (a) side surface of the castellation with a narrow deposition belt at the entrance to the gap; (b) schematic view of a castellated structure; (c) deposition profiles of D and metals in the castellation; note the plotted metal contents are magnified by a factor of 1000.

^{3}He-based NRA is extremely efficient in D studies on PFC surfaces. However, the assessment of global inventory requires knowledge of all hydrogen isotopes. Protium, though not used as a regular fuel in JET, is of interest because of possible H-D isotope exchange especially if an experimental campaign is finished with hydrogen discharges in order to clean the wall. Development and availability of protium analyses methods is strongly motivated by the fact that in the first phase of CFD operation H fueling is used to avoid immediate activation of components: Wendelstain-7X stellarator [60], also planned in JT60-SA and ITER. Protium analysis with ^{15}N(p, αγγ)^{12}C is limited to a small depth of less than 1 μm and, the quantification suffers from significant ion-induced detrapping of the analysed isotope. The aim is to measure H and D simultaneously within the same surface layer. Plots in Figure 6 (a-d) show ToF-HIERDA (42 MeV $^{127}I^{9+}$ beam) spectra and depth profiles recorded for the initial (a-b) and exposed (c-d) beryllium-coated Inconel®

tiles from the inner wall cladding of JET-ILW. The initial Be coating contains oxygen (10% at the very surface and 3-4% in depth) as the main impurity. Carbon and aluminum (Al source is unknown) are on the level of 1%. In the exposed plate one detects gettered oxygen (20-40%) and co-deposited H, D, C, N. Hydrogen is clearly detected. Its content is greater than that of D, because the campaign was finished with 300 discharges fueled with H [59,61,62].

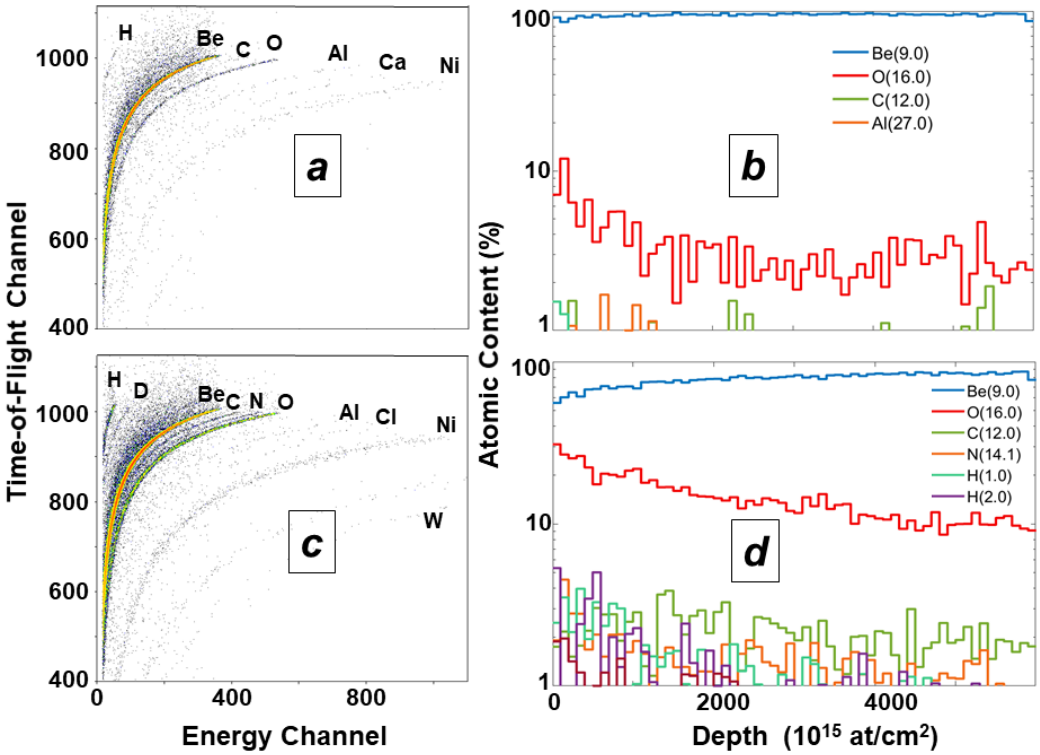

Fig. 6. ToF-HIERDA spectra and depth profiles of species in the surface region of Be coatings from the inner wall cladding of JET-ILW: (a) and (b) initial not exposed surfaces; (c) and (d) after exposure during the first and second ILW campaign.

Figure 7 shows results obtained with ToF-HIERDA for a co-deposit on a Si plate of a dust monitor located in JET-ILW above the outer divertor [18]. The plate was exposed during the second ILW campaign. Be is the main element in the co-deposit. There is also a significant amount of Ni; its origin has been explained in [63]. Other species are clearly marked in the spectrum thus proving simultaneous detection of light and heavy constituents from H to W. This makes ToF-HIERDA extremely useful in studies of wall probes from JET-ILW where the thickness of co-deposits does not exceed 1 μm [57,58,64,65].

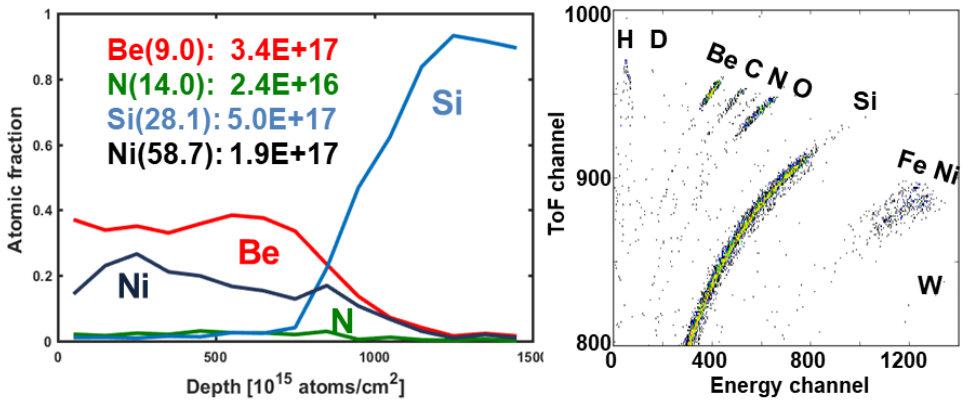

Fig. 7. ToF-HIERDA depth profile and spectrum of co-deposit on the silicon plate of the dust monitor in JET-ILW.

The overall objective of PFC analyses is obtain a global pattern of material migration and fuel retention. The main factor limiting the extent of studies is the availability of a large number of wall tiles and probes. The access to such reservoir is possible only at the end-of-life of a given machine, i.e. at the decommissioning phase. This was the case of the TEXTOR tokamak when a large number of tiles from different limiters could be retrieved and examined [66-68]. Deuterium content was measured around the torus in order to draw a retention map of all PFCs: toroidal belt limiter ALT II composed of eight blades, inner bumper limiter acting as a shield of the ergodig dynamic divertor and poloidal limiters, as shown in Figure 8. NRA measurements were performed with a 2.8 MeV $^{3}He^{+}$ beam enabling depth profiling to the depth of 10 μm. Numerical methods used for the interpolation are explained in [67,68] On most ALTII limiter tiles the deuterium is retained within the first 1-2 μm, with maximum concentration around 4-6% of the material mixture. On the bumper limiter, the deuterium is depleted in the first μm, peaks at ca. 2 μm, and falls off slowly with a measurable D content down to maximum 9 μm. The concentration maxima scatter between 2 and 12% of the material mixture. In summary, these comprehensive analyses have shown that after the last experimental campaign of TEXTOR, the bumper limiter had the highest surface concentration of fuel (average: 3.2×10^{18} cm^{-2}), while the average D content on ALTII (the main PFC of TEXTOR), was at the level of 0.4×10^{18} cm^{-2}).

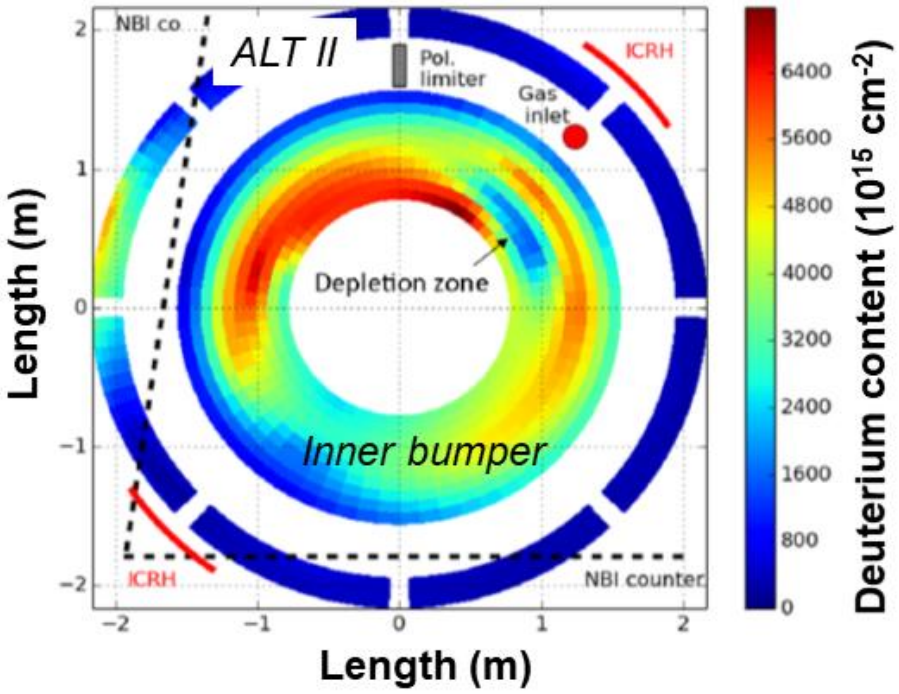

Fig. 8. Mapping of total deuterium content on the PFC of TEXTOR.

6. Ion-induced detrapping

Ion-induced release (detrapping) of H isotopes by the high-energy analyzing beam is to be taken into account in the quantification of retained fuel [26,64,69]. Therefore, D analysis should be performed with a relatively small $^3He^+$ dose (0.2 - 1 μC), unless the detrapping process itself is studied. The effective cross-sections for detrapping depend on the layer structure and its chemical composition, i.e. hybridisation, content of various plasma impurities in co-deposits, etc, as discussed in [70]. The substrate temperature also plays a role in the layer growth.

Figure 9(a) shows the change in the D depth profile and content in a co-deposit irradiated with an increasing dose of the 1.5 MeV $^3He^+$ beam: 4.7×10^{14} (A), 23.4×10^{15} (B) and 46.8×10^{15} cm^{-2} (C). They are recorded for a co-deposit formed on a collector probe exposed to the edge plasma at TEXTOR during discharges heated by neutral beam injection. The depth profiles prove a gradual but substantial release of D by over 45% from 2.6×10^{18} cm^{-2} to 1.4×10^{18} cm^{-2}. The decrease is not uniform: over 50% is released from the deepest region of the deposit; 35% from the middle layer (0.5–1.5 μm) and only about 5% from the surface region. The D release by MeV ^3He ions occurs mostly via electronic excitations. The effect is pronounced at the depth, where the $^3He^+$ energy is deposited most effectively. As shown in Figure 9(b) the electronic stopping power of 1.5 MeV ^3He ions in carbon matrix increases with depth reaching its maximum between 3 and 4 μm, i.e. in the region where the most effective detrapping has occurred.

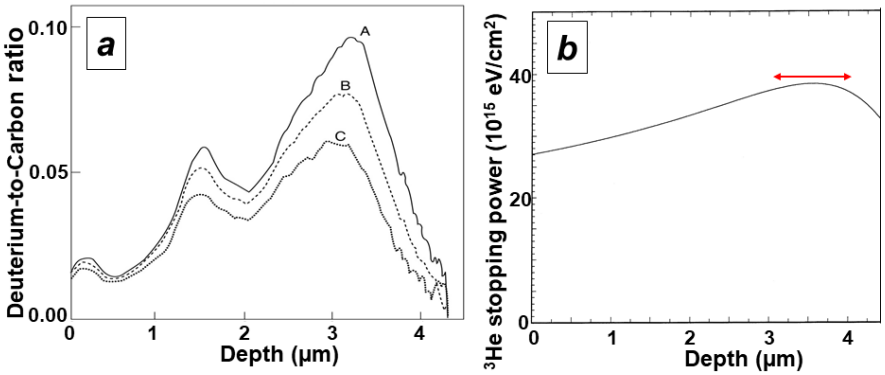

Fig. 9. Ion-induced release of D from co-deposits studied with ^{3}He-NRA: (a) the change of D depth profiles with the increased ion dose; (b) ^{3}He electronic stopping in a carbon target.

7. Concluding Remarks

In a brief synopsis, as presented above, only some topics and applications of IBA in studies of fusion reactor materials could be addressed. The methods, with all inherent advantages and also serious limitations, provide the most effective toolbox in PFC analyses from present-day devices. To meet contemporary research requirements continuous development of analytical tools takes place both at academic institutions and specialised industrial companies. In turn, such advances widen experimental capabilities especially in material migration studies (use of tracers) and in laboratory-based research under controlled conditions, e.g. interaction between hydrogen and candidates for wall materials. The latter requires chambers for in-situ experiments (e.g. exposure to plasma, implantation, thermal treatment) with simultaneous analyses to determine the dynamics of processes without breaking vacuum. In-situ IBA, i.e. inside the reactor has been discussed for long and, once it has been demonstrated in Alcator-C Mod [71]. However, such approach in a reactor-class machine will not be possible. IBA techniques play crucial role in the preparation and calibration of laser-based in-situ diagnosis of fuel retention [72] and, they will be essential in PFC analyses after deuterium-tritium campaigns.

Acknowledgements

This work was carried out within the framework of the EUROfusion consortium and has received funding from the Euratom research and training programme 2014–2018 and 2019–2020 under Grant Agreement No. 633053. The work has been supported by the Swedish Research Council (VR), Grant 2015–04844. Financial support of the Tandem Accelerator Infrastructure by VR-RFI (contract #2017-00646_9) as well as the Swedish Foundation for Strategic Research (SSF) under contract RIF14-0053 is gratefully acknowledged.

REFERENCES

1. Litaudon X. et al., **Overview of the JET in support of ITER,** *Nucl. Fusion* **2017**, *57*, 102001. https://doi.org/10.1088/1741-4326/aa5e28

2. Loarte A. et al., Power and particle control, Nucl. Fusion **2007**, *47*, S203-S263. https://doi.org/10.1088/0029-5515/47/6/S04
3. Federici G. et al., Plasma-material interactions in current tokamaks and their implications for next step fusion reactors, *Nucl. Fusion* **2001,** *41,* 1967-2137. https://doi.org/10.1088/0029-5515/41/12/218
4. Linke J., Plasma facing materials and components for future fusion devices—development, characterization and performance under fusion specific loading conditions *Phys. Scr.* **2006,** *T123,* 45-53. https://doi.org/10.1088/0031-8949/2006/T123/006
5. Matthews G.F. et al., *ITER-Like Wall Project overview, Phys. Scr.* **2007,** *T128*, 137-143. 10.1088/0031-8949/2007/T128/027
6. Bosch H-S., Halle G.M., Improved formulas for fusion cross-sections and thermal reactivities, *Nucl. Fusion* **1992**, *32*, 611-632. http://iopscience.iop.org/article/10.1088/0029-5515/32/4/I07/pdf
7. Tanabe T. (Ed), Tritium: Fuel of fusion reactors, *Springer Verlag,* **2016**.
8. Rubel M., Fusion Neutrons: Tritium breeding and impact on wall materials and components of diagnostic systems, *J. Fusion Energy* **2019**, 38, 315-329.
9. Baluc N., Materials for fusion power reactors, *Plasma Phys. Control. Fusion* **2006**, *48*, B165-B178. doi:10.1088/0741-3335/48/12B/S16
10. Neustroev V.S., Garner F.A., Severe embrittlement of neutron irradiated austenitic steels arising from high void swelling, *J. Nucl. Mater.* **2009**, *386-388*, 157-160. https://doi.org/10.1016/j.jnucmat.2008.12.077
11. Naujoks D., *Plasma-Material Interactions in Controlled Fusion, Springer Verlag,* **2006**.
12. Hofer W.O., Roth J. (Eds), Physical Processes of the Interaction of Fusion Plasmas with Solids, *Academic Press,* New York, 1996.
13. Philipps V., Wienhold P., Kirschner A., Rubel M., Erosion and redeposition of wall material in controlled fusion devices, *Vacuum* **2002**, *67*, 399-408. DOI: 10.1016/S0042-207X(02)00238-
14. Behrisch R. (Ed.), Sputtering by Particle Bombardment, *Springer Verlag*, 1981.
15. Roth J. et al., Tritium inventory in ITER plasma-facing materials and tritium removal procedures, *Plasma Phys. Control. Fusion* **2008**, 50, 103001. https://doi.org/10.1088/0741-3335/50/10/103001
16. Roth J. et al., Recent analysis of key plasma-wall interaction parameters for ITER, *J. Nucl. Mater.* **2009**, *390-391,* 1-9. https://doi.org/10.1016/j.jnucmat.2009.01.037
17. Counsell G.C., Tritium retention in next step devices and the requirements for mitigation and removal techniques, Plasma Phys. Control. Fusion **2006**, *48*, B189-B199. doi:10.1088/0741-3335/48/12B/S18

18. Rubel M. et al., Dust generation in tokamaks: Overview of beryllium and tungsten dust characterisation in JET with the ITER-like wall, Fusion Eng. Des. **2018**, *136*, 579-586. https://doi.org/10.1016/j.fusengdes.2018.03.027
19. Otsuka T et al., Tritium retention characteristics in dust particles in JET with ITER-like wall, *Nucl. Mater. Energy* **2018**, *17*, 279-286. https://doi.org/10.1016/j.nme.2018.11.001
20. Coad J.P. et al., Erosion/deposition issues in JET, *J. Nucl. Mater.* **2001,** *290-293*, 224-230. https://doi.org/10.1016/S0022-3115(00)00479-7
21. Tsitrone E. et al., Multi machine scaling of fuel retention in 4 carbon dominated tokamaks, *J. Nucl. Mater.* **2011**, *415*, S735-S739. doi:10.1016/j.jnucmat.2011.01.132
22. Skinner C.H. et al., Tritium experience in large tokamaks: Application to ITER, *Nucl. Fusion* **1999**, *39*, 271-292. https://doi.org/10.1088/0029-5515/39/2/410
23. Allen S.L. et al., ^{13}C transport studies in L-mode divertor plasmas on DIII-D, *J. Nucl. Mater.* **2005**, *337-339*, 30-34. doi:10.1016/j.jnucmat.2004.09.066
24. Loarer T. et al., Gas balance and fuel retention in fusion devices, *Nucl. Fusion* **2007**, *47*, 1112-1120. doi:10.1088/0029-5515/47/9/007
25. Penzhorn R-D. et al., Tritium depth profiles in graphite and carbon fibre composite material exposed to tokamak plasmas, *J. Nucl. Mater.* **2001,** *288*, 170-178. https://doi.org/10.1016/S0022-3115(00)00705-4
26. M. Rubel et al., Beryllium and carbon films in JET following D-T operation, *J. Nucl. Mater.* **2003**, *313-316*, 321-326. https://doi.org/101016/S0022-3115(02)01350-8
27. Matthews G.F. et al., JET ITER-Like Wall: Overview of experimental program, *Phys. Scr.* **2011,** *T145*, 014001. 10.1088/0031-8949/2007/T128/027
28. Coad J.P. et al. Material migration and fuel retention studies during the JET carbon divertor campaigns, *Fusion Engin. Design* **2018**, 138, 78-108. https://doi.org/10.1016/j.fusengdes.2018.10.002
29. Maier H. et al., Tungsten and beryllium armour development for the JET ITER-like wall Project, *Nucl. Fusion* **2007**, *47*, 222-227. doi:10.1088/0029-5515/47/3/009
30. Rubel M. et al., Beryllium plasma-facing components for the ITER-Like Wall Project at JET, *J. Phys. Conf. Series* **2008**, *100*, 062028. doi:10.1088/1742-6596/100/6/062028
31. Mertens Ph. et al., Clamping of solid tungsten components for the bulk W divertor row in JET—precautionary design for a brittle material, *Phys. Scr.* **2009**, *T138*, 014032. https://doi.org/10.1088/0031-8949/2009/T138/014032
32. Mertens Ph. et al., Detailed design of a solid tungsten divertor row for JET in relation to the physics goals, *Phys. Scr.* **2011**, *T145*, 014002. https://doi.org/10.1088/0031-8949/2011/T145/014002
33. Matthews G.F. et al., Current status of the JET ITER-like Wall Project, *Phys. Scr.* **2010**, *T138*, 014030. doi:10.1088/0031-8949/2009/T138/014030

34. Matthews G.F., Plasma operation with an all metal first-wall: Comparison of an ITER-like wall with a carbon wall in JET, *J. Nucl. Mater.* **2013,** *438* S2-S10. https://doi.org/10.1016/j.jnucmat.2013.01.282
35. Loarer T. et al., Comparison of fuel retention in JET between carbon and the ITER-Like Wall, *J. Nucl. Mater.* **2013**, *438*, S108-S113. https://doi.org/10.1016/j.jnucmat.2013.01.017
36. Brezinsek S. et al., Beryllium migration in JET ITER-like wall Plasmas, *Nucl. Fusion* **2015**, *55,* 063021. doi:10.1088/0029-5515/55/6/063021
37. Merola M., et al., Overview and status of ITER internal components, *Fusion Eng. Des*. **2014**, *89*, 890-895. https://doi.org/10.1016/j.fusengdes.2014.01.055
38. Widdowson A. et al., Experience of handling beryllium, tritium and activated components from JET ITER like wall, *Phys. Scr.* **2016**, *T167*, 014057. doi:10.1088/0031-8949/T167/1/014057
39. Rubel M, Analysis of plasma facing materials: material migration and fuel retention, *Phys. Scr.* **2006**, *T123*, 54-65. doi:10.1088/0031-8949/2006/T123/007
40. Rubel M. et al., The role and application of ion beam analysis for studies of plasma-facing components in controlled fusion devices, *Nucl. Instr. Meth.* **2016,** *B371,* 4-11. http://dx.doi.org/10.1016/j.nimb.2015.09.077
41. Chu W.K., Mayer M., Nicolet M.A., Backscattering Spectroscopy, *Academic Press*, New York, **1978.**
42. Tesmer J.R., Nastasi M. (Eds), Handbook of Modern Ion Beam Analysis, *Material Research Society*, **1995,** Pittsburg, PA.
43. Mayer M. et al., Ion beam analysis of fusion plasma-facing materials and components: facilities and research challenges, *Nucl. Fusion* **2020**, *60*, 025001. https://doi.org/10.1088/1741-4326/ab5817
44. Mayer M. et al., Quantitative depth profiling of deuterium up to very large depths, *Nucl. Instr. Meth.* **2009,** *B267,* 506-512. https://doi.org/10.1016/j.nimb.2008.11.033
45. Kantre K. et al., Combination of in-situ ion beam analysis and thermal desorption spectroscopy for studying deuterium implanted in tungsten, *Phys. Scr.* **2021**, *96*, 124004. https://doi.org/10.1088/1402-4896/ac1a88
46. Ström P., Petersson P., Rubel M., Possnert G., A combined segmented anode gas ionization chamber and time-of-flight detector for heavy ion elastic recoil detection analysis, *Rev. Sci. Instrum.* **2016**, *87*, 103303. http://dx.doi.org/10.1063/1.4963709
47. Mayer M. *SIMNRA Users Guide, Report IPP 9/113*, Garching: Max-Planck-Institut für Plasmaphysik, **1997.**
48. Rubel M. et al., Overview of tracer techniques in studies of material erosion, re-deposition and fuel inventory in tokamaks, *J. Nucl. Mater.* **2004,** *329-333***,** 795-799. doi:10.1016/j.jnucmat.2004.04.154

49. Coad J.P. et al., Overview of material re-deposition and Fuel retention studies at JET with the Gas Box divertor, *Nucl. Fusion* **2006**, *46*, 350-366. doi:10.1088/0029-5515/46/2/018
50. Heinola K. et al., Long-term fuel retention in JET ITER-like wall, *Phys. Scr.* **2016**, *T167*, 014075. https://doi.org/10.1088/0031-8949/T167/1/014075
51. Heinola K. et al., Experience on divertor fuel retention after two ITER-Like Wall campaigns, *Phys. Scr.* **2017**, *T170,* 014063 https://doi.org/10.1088/1402-4896/aa9283
52. Mayer M. et al., Erosion and deposition in the JET divertor during the first ILW campaign, *Phys. Scr.* **2016**, *T167*, 014051. https://doi.org/10.1088/0031-8949/T167/1/014051
53. Widdowson A. et al., Overview of fuel inventory in JET with the ITER-like wall, *Nucl. Fusion* **2017**, *57*, 086045. https://doi.org/10.1088/1741-4326/aa7475
54. Widdowson A. et al., Overview of the JET ITER-like wall divertor, *Nucl. Mater. Energy* **2017**, *12*, 499-505. https://doi.org/10.1016/j.nme.2016.12.008
55. Widdowson A. et al., Fuel inventory and material migration of JETmain chamber plasma facing components compared over three operational periods, *Phys. Scr.* **202**0, *T171*, 014051. https://doi.org/10.1088/1402-4896/ab5350
56. Krat S. et al., Comparison of erosion and deposition in JET divertor during the first three ITER-like wall campaigns, *Phys. Scr.* **2020**, *T171*, 014059. https://doi.org/10.1088/1402-4896/ab5c11
57. Ivanova D. et al., An overview of the Comprehensive First Mirrors Test in JET with ITER-Like Wall, *Phys. Scr.* **2014**, *T159*, 014011. doi:10.1088/0031-8949/2014/T159/014011
58. Moon Sunwoo et al., First mirror test in JET for ITER: Complete overview after three ILW campaigns, *Nucl. Mater. Energy* **2019**, *19*, 59-66. https://doi.org/10.1016/j.nme.2019.02.009
59. Rubel M. et al., Fuel inventory and deposition in castellated structures in JET-ILW, *Nucl. Fusion* **2017,** *57*, 066027. https://doi.org/10.1088/1741-4326/aa6864
60. Brezinsek S. et al., Plasma-Surface Interaction in the Stellarator W7-X: Conclusion Drawn from Operation with Graphite Plasma-Facing Components, *Nucl. Fusion* **2021** https://doi.org/10.1088/1741-4326/ac3508
61. Dittrich L. et al., Fuel retention and erosion-deposition on inner wall cladding tiles in JET-ILW, *Phys. Scr.* https://doi.org/10.1088/1402-4896/ac379e
62. Widdowson A. et al., Evaluation of tritium retention in plasma facing components during JET tritium operations, *Phys. Scr.* in press.
63. Widdowson A., et al., Deposition of impurity metals during campaigns with the JET ITER-like Wall, *Nucl. Mater. Energy* **2019**, *19*, 218-224. https://doi.org/10.1016/j.nme.2018.12.024
64. Ström P. et al., Analysis of co-deposited layers with deuterium and impurity elements on samples from the divertor of JET with ITER-like wall, *J. Nucl. Mater*. **2019**, *516*, 202-213. https://doi.org/10.1016/j.jnucmat.2018.11.027

65. Rubel M. et al., First mirror erosion-deposition studies in JET using an ITER-like mirror test assembly, *Nucl. Fusion* **2021**, *61*, 046022. https://doi.org/10.1088/1741-4326/abdb92

66. Weckmann A. et al., Whole-machine material migration studies in the TEXTOR tokamak with molybdenum, *Nucl. Mater. Energy*, **2017**, *12*, 518-523. http://dx.doi.org/10.1016/j.nme.2016.12.011

67. Weckmann A. et al., Review of global migration, fuel retention and modelling after TEXTOR decommission, *Nucl. Mater. Energy*, **2018**, *17*, 83-112. https://doi.org/10.1016/j.nme.2018.09.003

68. Weckmann A., Material migration in tokamaks. Erosion-deposition patterns and transport processes, *Ph.D. Thesis, KTH Royal Institute of Technology*, **2017**, ISBN: 978-91-7729-461-0

69. Rubel M., Bergsåker H., Wienhold P., Ion-induced release of deuterium from co-deposits by high-energy helium bombardment, *J. Nucl. Mater*. **1997**, *241-243*, 1026-1030. doi:10.1016/S0022-3115(97)80187-0

70. Rubel M, Coad J.P., Likonen J., Philipps V., Analysis of fuel retention in plasma-facing components from controlled fusion devices, *Nucl. Instrum. Meth.* **2009**, *B267*, 711-717. http://dx.doi.org/10.1016/j.nimb.2008.11.035

71. Hartwig Z.S. et al., Fuel retention measurements in Alcator C-Mod using accelerator-based in situ materials surveillance, *J. Nucl. Mater*. **2015**, 463, 73-77. doi: 10.1016/j.jnucmat.2014.09.056

72. Philipps V. et al., Development of Laser Based Techniques for In-Situ Characterization of the First Wall in ITER and Future Fusion Devices, *Nucl. Fusion* **2013**, *53*, 093002. doi:10.1088/0029-5515/53/9/093002